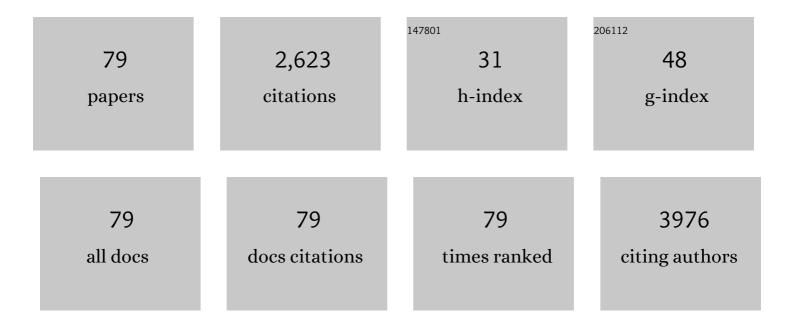
## Yong Zhang

List of Publications by Year in descending order

Source: https://exaly.com/author-pdf/6044445/publications.pdf

Version: 2024-02-01



YONG ZHANG

#	Article	IF	CITATIONS
1	Nanoporous carbon nanowires derived from one-dimensional metal-organic framework core-shell hybrids for enhanced electrochemical energy storage. Applied Surface Science, 2022, 576, 151800.	6.1	9
2	Pseudocapacitive TiNb2O7/reduced graphene oxide nanocomposite for high–rate lithium ion hybrid capacitors. Journal of Colloid and Interface Science, 2022, 610, 385-394.	9.4	11
3	High-yielding preparation of hierarchically branched carbon nanotubes derived from zeolitic imidazolate frameworks for enhanced electrochemical K <sup>+</sup> storage. Dalton Transactions, 2022, 51, 5441-5447.	3.3	4
4	Ti <sub>3</sub> AlC <sub>2</sub> MAX and Ti <sub>3</sub> C <sub>2</sub> MXene Quantum Sheets for Record-High Optical Nonlinearity. Journal of Physical Chemistry Letters, 2022, 13, 3929-3936.	4.6	7
5	In situ W/O Co-doped hollow carbon nitride tubular structures with enhanced visible-light-driven photocatalytic performance for hydrogen evolution. International Journal of Hydrogen Energy, 2021, 46, 234-246.	7.1	19
6	Controlled growth of porous oxygen-deficient NiCo <sub>2</sub> O <sub>4</sub> nanobelts as high-efficiency electrocatalysts for oxygen evolution reaction. Catalysis Science and Technology, 2021, 11, 264-271.	4.1	11
7	A general strategy for semiconductor quantum dot production. Nanoscale, 2021, 13, 8004-8011.	5.6	13
8	Designed Construction of SrTiO <sub>3</sub> /SrSO <sub>4</sub> /Pt Heterojunctions with Boosted Photocatalytic H <sub>2</sub> Evolution Activity. Chemistry - A European Journal, 2021, 27, 7300-7306.	3.3	12
9	Carbon Nanolayer-Wrapped Mesoporous TiO <sub>2</sub> –B/Anatase for Li <sup>+</sup> Storage. ACS Applied Nano Materials, 2021, 4, 7832-7839.	5.0	8
10	Scalable production of intrinsic WX <sub>2</sub> (XÂ=ÂS, Se, Te) quantum sheets for efficient hydrogen evolution electrocatalysis. Nanotechnology, 2021, 32, 495701.	2.6	10
11	Designing core–shell metal–organic framework hybrids: toward high-efficiency electrochemical potassium storage. Journal of Materials Chemistry A, 2021, 9, 26181-26188.	10.3	10
12	Tunable Synthesis of 3D Niobium Oxynitride Nanosheets for Lithium-Ion Hybrid Capacitors with High Energy/Power Density. ACS Sustainable Chemistry and Engineering, 2021, 9, 14569-14578.	6.7	7
13	Hierarchical NiCo2O4/MnO2 core–shell nanosheets arrays for flexible asymmetric supercapacitor. Journal of Materials Science, 2020, 55, 688-700.	3.7	31
14	Fabrication of WO3/TiO2 core-shell nanowire arrays: Structure design and high electrochromic performance. Electrochimica Acta, 2020, 330, 135189.	5.2	34
15	PEDOT hollow nanospheres for integrated bifunctional electrochromic supercapacitors. Organic Electronics, 2020, 77, 105497.	2.6	28
16	A surface precleaning strategy intensifies the interface coupling of the Bi <sub>2</sub> O <sub>3</sub> /TiO <sub>2</sub> heterostructure for enhanced photoelectrochemical detection properties. Materials Chemistry Frontiers, 2020, 4, 638-644.	5.9	9
17	Effect of conductive PANI vs. insulative PS shell coated Ni nanochains on electromagnetic wave absorption. Journal of Alloys and Compounds, 2020, 821, 153531.	5.5	18
18	Metal-organic framework-derived porous Cu2O/Cu@C core-shell nanowires and their application in uric acid biosensor. Applied Surface Science, 2020, 506, 144662.	6.1	18

YONG ZHANG

#	Article	IF	CITATIONS
19	Controlled Production of MoS <sub>2</sub> Full‧cale Nanosheets and Their Strong Size Effects. Advanced Materials Interfaces, 2020, 7, 2001130.	3.7	17
20	CoO Quantum Dots Anchored on Reduced Graphene Oxide Aerogels for Lithium-Ion Storage. ACS Applied Nano Materials, 2020, 3, 10369-10379.	5.0	16
21	Tuning Morphology and Electronic Structure of Amorphous NiFeB Nanosheets for Enhanced Electrocatalytic N <sub>2</sub> Reduction. ACS Applied Energy Materials, 2020, 3, 9516-9522.	5.1	16
22	Graphene quantum dots interfacial-decorated hierarchical Ni/PS core/shell nanocapsules for tunable microwave absorption. Journal of Alloys and Compounds, 2020, 848, 156529.	5.5	12
23	Tailoring Multi-Walled Carbon Nanotubes into Graphene Quantum Sheets. ACS Applied Materials & Interfaces, 2020, 12, 47784-47791.	8.0	10
24	Synthesis of SrTiO <sub>3</sub> submicron cubes with simultaneous and competitive photocatalytic activity for H <sub>2</sub> O splitting and CO <sub>2</sub> reduction. RSC Advances, 2020, 10, 42619-42627.	3.6	10
25	Construction of three-dimensional hierarchical Pt/TiO2@C nanowires with enhanced methanol oxidation properties. International Journal of Hydrogen Energy, 2020, 45, 33440-33447.	7.1	12
26	Enhanced Oxygen Reduction Catalysis of Carbon Nanohybrids from Nitrogen-Rich Edges. Langmuir, 2020, 36, 13752-13758.	3.5	5
27	Rational construction of porous amorphous WO3 nanostructures with high electrochromic energy storage performance: Effect of temperature. Journal of Non-Crystalline Solids, 2020, 549, 120337.	3.1	12
28	Directly Exfoliated Ultrathin Silicon Nanosheets for Enhanced Photocatalytic Hydrogen Production. Journal of Physical Chemistry Letters, 2020, 11, 8668-8674.	4.6	14
29	Carbon-Coated Self-Assembled Ultrathin T-Nb <sub>2</sub> O <sub>5</sub> Nanosheets for High-Rate Lithium-Ion Storage with Superior Cycling Stability. ACS Applied Energy Materials, 2020, 3, 12037-12045.	5.1	26
30	Enhanced Energy Storage Performance of 3D Hybrid Metal Sulfides via Synergistic Engineering of Architecture and Composition. ACS Sustainable Chemistry and Engineering, 2020, 8, 11491-11500.	6.7	5
31	Self-assembly of 0D/2D homostructure for enhanced hydrogen evolution. Materials Today, 2020, 36, 83-90.	14.2	24
32	Rational Design of Oxygen Deficiency-Controlled Tungsten Oxide Electrochromic Films with an Exceptional Memory Effect. ACS Applied Materials & Interfaces, 2020, 12, 32658-32665.	8.0	46
33	A solvent-assisted ligand exchange approach enables metal-organic frameworks with diverse and complex architectures. Nature Communications, 2020, 11, 927.	12.8	93
34	MoS2 quantum dots decorated ultrathin NiO nanosheets for overall water splitting. Journal of Colloid and Interface Science, 2020, 566, 411-418.	9.4	38
35	Structure modulated amorphous/crystalline WO3 nanoporous arrays with superior electrochromic energy storage performance. Solar Energy Materials and Solar Cells, 2020, 212, 110579.	6.2	45
36	Ultrathin carbon coated mesoporous Ni-NiFe2O4 nanosheet arrays for efficient overall water splitting. Electrochimica Acta, 2019, 321, 134652.	5.2	37

Yong Zhang

#	Article	IF	CITATIONS
37	Construction of WO3/Ti-doped WO3 bi-layer nanopore arrays with superior electrochromic and capacitive performances. Tungsten, 2019, 1, 236-244.	4.8	7
38	Hierarchical Hybrid of Few-Layer Graphene upon Tungsten Monocarbide Nanowires: Controlled Synthesis and Electrocatalytic Performance for Methanol Oxidation. ACS Applied Energy Materials, 2019, 2, 328-337.	5.1	3
39	3D carbon coated NiCo2S4 nanowires doped with nitrogen for electrochemical energy storage and conversion. Journal of Colloid and Interface Science, 2019, 556, 449-457.	9.4	37
40	Crystalline WO3 nanowires array sheathed with sputtered amorphous shells for enhanced electrochromic performance. Applied Surface Science, 2019, 498, 143796.	6.1	42
41	Fabrication of CoFe/N-doped mesoporous carbon hybrids from Prussian blue analogous as high performance cathodes for lithium-sulfur batteries. International Journal of Hydrogen Energy, 2019, 44, 20257-20266.	7.1	20
42	Water-Soluble Defect-Rich MoS <sub>2</sub> Ultrathin Nanosheets for Enhanced Hydrogen Evolution. Journal of Physical Chemistry Letters, 2019, 10, 3282-3289.	4.6	50
43	Robust production of 2D quantum sheets from bulk layered materials. Materials Horizons, 2019, 6, 1416-1424.	12.2	28
44	Nitrogen, sulfur-codoped micro–mesoporous carbon derived from boat-fruited sterculia seed for robust lithium–sulfur batteries. RSC Advances, 2019, 9, 15715-15726.	3.6	24
45	Z-scheme carbon-bridged Bi2O3/TiO2 nanotube arrays to boost photoelectrochemical detection performance. Applied Catalysis B: Environmental, 2019, 248, 255-263.	20.2	85
46	Hydrothermal synthesis of well-standing δ-MnO2 nanoplatelets on nitrogen-doped reduced graphene oxide for high-performance supercapacitor. Journal of Alloys and Compounds, 2019, 787, 309-317.	5.5	19
47	Designed growth of WO3/PEDOT core/shell hybrid nanorod arrays with modulated electrochromic properties. Chemical Engineering Journal, 2019, 355, 942-951.	12.7	72
48	<i>In situ</i> growth of PEDOT/graphene oxide nanostructures with enhanced electrochromic performance. RSC Advances, 2018, 8, 13679-13685.	3.6	41
49	In-situ construction of NiCo2O4 nanoarrays on La0.8Sr0.2MnO3-δ electrodes for intermediate temperature solid oxide fuel cells. Journal of Solid State Electrochemistry, 2018, 22, 2367-2374.	2.5	0
50	Supercapacitive performance of single phase CuO nanosheet arrays with ultra-long cycling stability. Journal of Alloys and Compounds, 2018, 753, 731-739.	5.5	10
51	MOF-74 derived porous hybrid metal oxide hollow nanowires for high-performance electrochemical energy storage. Journal of Materials Chemistry A, 2018, 6, 8396-8404.	10.3	101
52	Enhanced photocatalytic performances of ultrafine g-C3N4 nanosheets obtained by gaseous stripping with wet nitrogen. Applied Surface Science, 2018, 427, 730-738.	6.1	47
53	CeO <sub>2â^'x</sub> /C/rGO nanocomposites derived from Ce-MOF and graphene oxide as a robust platform for highly sensitive uric acid detection. Nanoscale, 2018, 10, 1939-1945.	5.6	88
54	Preparation of V <sub>2</sub> O <sub>5</sub> dot-decorated WO <sub>3</sub> nanorod arrays for high performance multi-color electrochromic devices. Journal of Materials Chemistry C, 2018, 6, 12206-12216.	5.5	31

Yong Zhang

#	Article	IF	CITATIONS
55	In-situ synthesis of carbon-coated β-NiS nanocrystals for hydrogen evolution reaction in both acidic and alkaline solution. International Journal of Hydrogen Energy, 2018, 43, 16061-16067.	7.1	11
56	Controlled synthesis of MnO2@TiO2 hybrid nanotube arrays with enhanced oxygen evolutionÂreaction performance. International Journal of Hydrogen Energy, 2018, 43, 14369-14378.	7.1	22
57	3D Coral-Like Ni <sub>3</sub> S <sub>2</sub> on Ni Foam as a Bifunctional Electrocatalyst for Overall Water Splitting. ACS Applied Materials & Interfaces, 2018, 10, 31330-31339.	8.0	80
58	In-situ constructing NiO nanoplatelets network on La 0.75 Sr 0.25 Mn 0.5 Cr 0.5 O 3-δ electrode with enhanced steam electrolysis. International Journal of Hydrogen Energy, 2017, 42, 5657-5666.	7.1	4
59	Synthesis of W2N nanorods-graphene hybrid structure with enhanced oxygen reduction reaction performance. International Journal of Hydrogen Energy, 2017, 42, 25924-25932.	7.1	14
60	Synthesis of α-Bi <sub>2</sub> Mo <sub>3</sub> O <sub>12</sub> /TiO <sub>2</sub> Nanotube Arrays for Photoelectrochemical COD Detection Application. Langmuir, 2017, 33, 8933-8942.	3.5	27
61	Cryo-mediated exfoliation and fracturing of layered materials into 2D quantum dots. Science Advances, 2017, 3, e1701500.	10.3	91
62	One-step electrodeposition of Co 0·12 Ni 1·88 S 2 @Co 8 S 9 nanoparticles on highly conductive TiO 2 nanotube arrays for battery-type electrodes with enhanced energy storage performance. Journal of Power Sources, 2017, 364, 400-409.	7.8	17
63	In-situ constructing hybrid oxygen electrode of porous Co3O4 nanowire array on La0.8Sr0.2MnO3â~δ for steam electrolysis. International Journal of Hydrogen Energy, 2016, 41, 5428-5436.	7.1	6
64	Size-Controlled TiO 2 nanocrystals with exposed {001} and {101} facets strongly linking to graphene oxide via p -Phenylenediamine for efficient photocatalytic degradation of fulvic acids. Journal of Hazardous Materials, 2016, 314, 41-50.	12.4	35
65	Construction of CuO/Cu2O@CoO core shell nanowire arrays for high-performance supercapacitors. Surface and Coatings Technology, 2016, 299, 15-21.	4.8	49
66	Integration of mesoporous nickel cobalt oxide nanosheets with ultrathin layer carbon wrapped TiO <sub>2</sub> nanotube arrays for high-performance supercapacitors. New Journal of Chemistry, 2016, 40, 6881-6889.	2.8	18
67	Hydrothermal synthesis of layered molybdenum sulfide/N-doped graphene hybrid with enhanced supercapacitor performance. Carbon, 2016, 99, 35-42.	10.3	183
68	Synthesis of porous NiO/CeO <sub>2</sub> hybrid nanoflake arrays as a platform for electrochemical biosensing. Nanoscale, 2016, 8, 770-774.	5.6	41
69	A high performance electrochemical biosensor based on Cu <sub>2</sub> O–carbon dots for selective and sensitive determination of dopamine in human serum. RSC Advances, 2015, 5, 54102-54108.	3.6	68
70	A facile synthesis of mesoporous Co <sub>3</sub> O <sub>4</sub> /CeO <sub>2</sub> hybrid nanowire arrays for high performance supercapacitors. Journal of Materials Chemistry A, 2015, 3, 10425-10431.	10.3	108
71	Chromate cathode decorated with in-situ growth of copper nanocatalyst for high temperature carbon dioxide electrolysis. International Journal of Hydrogen Energy, 2014, 39, 20888-20897.	7.1	54
72	Reversibly in-situ anchoring copper nanocatalyst inÂperovskite titanate cathode for direct high-temperature steam electrolysis. International Journal of Hydrogen Energy, 2014, 39, 5485-5496.	7.1	48

YONG ZHANG

#	Article	IF	CITATIONS
73	Size-dependent surface phase change of lithium iron phosphate during carbon coating. Nature Communications, 2014, 5, 3415.	12.8	66
74	Single-phase nickel-doped ceria cathode with in situ grown nickel nanocatalyst for direct high-temperature carbon dioxide electrolysis. RSC Advances, 2014, 4, 40494-40504.	3.6	26
75	Carbon-coated tungsten oxide nanowires supported Pt nanoparticles for oxygen reduction. International Journal of Hydrogen Energy, 2012, 37, 4633-4638.	7.1	33
76	3D boron doped carbon nanorods/carbon-microfiber hybrid composites: synthesis and applications in a highly stable proton exchange membrane fuel cell. Journal of Materials Chemistry, 2011, 21, 18195.	6.7	38
77	Synthesis and electrochemical properties of LSM and LSF perovskites as anode materials for high temperature steam electrolysis. Journal of Power Sources, 2009, 186, 485-489.	7.8	49
78	Tungsten oxide nanowires grown on carbon paper as Pt electrocatalyst support for high performance proton exchange membrane fuel cells. Journal of Power Sources, 2009, 192, 330-335.	7.8	84
79	Three-Dimensional Hierarchical Structure of Single Crystalline Tungsten Oxide Nanowires: Construction, Phase Transition, and Voltammetric Behavior. Journal of Physical Chemistry C, 2009, 113, 1746-1750.	3.1	49